



Effect of Biopolymer-Based Soil Treatment on Lateral Earth Pressure in Sandy Soil Backfill: An Experimental Study Utilizing a Laboratory-Scale Soil Tank Apparatus and PIV Analysis

Gi-Yun Kim¹; Suhyuk Park²; and Ilhan Chang, Ph.D., A.M.ASCE³

Abstract: Materials meeting stringent criteria for retaining wall backfill typically result in increased wall volume to resist Earth pressure, which consequently drives up construction costs. Recently, due to the depletion of natural construction resources, locally sourced soils and sustainable materials are being investigated as alternative backfill materials. Studies are performed aiming to efficiently reduce lateral earth pressure using suitable materials. One innovative method is biopolymer-based soil treatment (BPST), recognized as an environmentally friendly geotechnical binder that improves soil strength. This study aims to employ biopolymers in retaining wall backfills to mitigate environmental concerns associated with the use of traditional soil improvers like cement in geotechnical engineering. The investigation of lateral earth pressure behavior for backfill reinforcement conditions was performed through laboratory tests and particle image velocimetry (PIV) analysis, including the introduction of a rotatable wall (rotation around the base) to support sandy soil. XG-BPST was formulated based on sand mass, 15% deionized water, and 1% xanthan gum biopolymer content and was classified into initial (wet) or dehydrated (dry) conditions. To address the weak strength of the initial (wet) condition of XG-BPST, a geogrid was encapsulated in the center of the XG-BPST layer. The reduction of lateral earth pressure and stability verification of retaining walls were investigated on backfills reinforced with XG-BPST and geogrid. Laboratory tests demonstrated that wall displacement reached a limit equilibrium state of approximately $\Delta x/h$ 0.1% (active earth pressure), regardless of the backfill reinforcement conditions. In the initial (wet) state of XG-BPST, the variation in lateral earth pressure behavior was negligible compared to the untreated condition, due to a weak improvement in shear strength. However, significant reductions in lateral earth pressure were observed when the geogrid was integrated with the XG-BPST layer or in the dehydrated (dry) condition of XG-BPST, attributed to the restriction of ground deformation at the reinforcement position and the confinement effect on the surrounding soil. The laboratory test results confirmed that lowering active earth pressure enhances the external stability of the retaining wall. Moreover, the required wall width to satisfy safety guidelines decreased, indicating the feasibility of more economically efficient designs. DOI: 10.1061/JGGEFK.GTENG-13027. This work is made available under the terms of the Creative Commons Attribution 4.0 International license, <https://creativecommons.org/licenses/by/4.0/>.

Author keywords: Active earth pressure; Biopolymer-based soil treatment (BPST); External stability; Laboratory test; Lateral earth pressure; Retaining wall backfill; Rotation around the base; Xanthan gum biopolymer.

Introduction

The conventional earth pressure theories of Coulomb (1776) and Rankine (1857), which assume a planar sliding surface, are commonly used in retaining wall design and have proven to be reliable. However, research has shown that earth pressure distribution is nonlinear and depends on the wall displacement mode, such as translation or rotation around the top or base (Fang and Ishibashi

1986; Fang et al. 1994; Chang 1997). Since wall displacement affects backfill deformation and failure mechanisms, conventional earth pressure theories may not accurately assess lateral earth pressure (Rui et al. 2024). Physical modeling test at the laboratory scale provides enhanced control over wall displacement modes and enables precise measurement of earth pressure, yielding significant insights. Moreover, advanced technologies such as digital image correlation (DIC) and particle image velocimetry (PIV) have improved the monitoring of ground deformation during experiments, facilitating studies on backfill behavior under various wall displacement modes (Niedostatkiwicz et al. 2011; Khosravi et al. 2013; Patel and Deb 2020).

Generally, granular cohesionless backfill materials with adequate drainage and strength are preferred. However, to ensure resistance to lateral earth pressure, the volume of the retaining wall is increased by using existing backfill soils, which raises construction costs due to the need for more materials (Azzam and Abdelsalam 2015). Due to the scarcity of natural materials, the use of sustainable or locally available soils as alternatives is being investigated to reduce lateral earth pressure by incorporating suitable materials into the backfill (Reddy and Krishna 2015; Gade and Dasaka 2022). Studies have tested lightweight materials such as tire chips

¹Graduate Student, Dept. of Civil Systems Engineering, Ajou Univ., Suwon-Si 16499, Republic of Korea. ORCID: <https://orcid.org/0009-0008-8858-9409>. Email: kky950317@ajou.ac.kr

²Graduate Student, Dept. of Civil Systems Engineering, Ajou Univ., Suwon-Si 16499, Republic of Korea. ORCID: <https://orcid.org/0000-0003-4360-6902>. Email: phy9958@ajou.ac.kr

³Associate Professor, Dept. of Civil Systems Engineering, Ajou Univ., Suwon-Si 16499, Republic of Korea (corresponding author). ORCID: <https://orcid.org/0000-0001-8369-0606>. Email: ilhanchang@ajou.ac.kr

Note. This manuscript was submitted on May 15, 2024; approved on January 6, 2025; published online on April 28, 2025. Discussion period open until September 28, 2025; separate discussions must be submitted for individual papers. This technical note is part of the *Journal of Geotechnical and Geoenvironmental Engineering*, © ASCE, ISSN 1090-0241.

(Cecich et al. 1996; Tweedie et al. 1998; Reddy and Krishna 2015; Kaneda et al. 2018; Djadouni et al. 2021), compressible EPS geofoam (Horvath 1997; Ikizler et al. 2008; Ertugrul and Trandafir 2011; Ertugrul and Trandafir 2013; Azzam and Abdelsalam 2015; Ni et al. 2016; Khajeh et al. 2020; Gade and Dasaka 2022; Han et al. 2023), and relief shelves (Moon et al. 2013; Chauhan et al. 2016a, b; Khan et al. 2016; Chauhan Vinay and Dasaka 2018) to decrease wall volume and enhance stability, achieving more cost-effective designs (Khan et al. 2016).

Traditional soil improvement agents like cement, lime, and fly ash adversely affect the environment and contribute to climate change via CO₂ emissions. Consequently, research in geotechnical engineering has shifted toward developing eco-friendly and sustainable binders, such as biopolymer-based soil treatments (BPST). Dehydration of biopolymer hydrogel, accompanied by drying, enhances shear strength of BPST through surface coating and inter-particle bridging, which facilitated by the condensation of biopolymer biofilms (Chang et al. 2016a, 2020; Lee et al. 2017). The BPST provides engineering efficiency while meeting environmental protection standards and achieving carbon neutrality; however, further research is needed concerning site suitability, durability, constructability, and economic feasibility (Chang et al. 2020).

This study introduces a rotatable wall designed to evaluate the distribution of earth pressure at various depths within sandy soil. The behavior of lateral pressure under diverse backfill conditions, including variations in BPST layers, was analyzed using mechanical instruments (load transducers and earth pressure gauges) and the image analysis method (GeoPIV).

Materials

Jumunjin Sand

The main soil used in this study was Jumunjin sand, a cohesionless dry granular soil with high sphericity and low fine-grained content. The physical properties of Jumunjin sand were assessed using ASTM standards and summarized in Fig. 1 and Table 1.

Xanthan Gum Biopolymer

BPST may produce biopolymers via ex-situ (exo-cultivation) methods, allowing for enhanced quality control compared to other biological soil treatment technologies. Additionally, biopolymers can be commercially mass-produced and combined with soil particles postmixing for temporary or rapid support purposes (Chang et al. 2016b). In this study, purified xanthan gum biopolymer (Sigma-Aldrich, CAS No. 11138-66-2) was dissolved in deionized water to form a hydrogel solution, which was subsequently mixed with sand to make a xanthan gum (XG)-sand mixture (BPST) (hereafter, XG-BPST). Literature reviews on recent studies of xanthan gum biopolymer have reported various results concerning soil improvement effect and behavior at 1% m_b/m_s concentration. To prepare the XG-BPST sample, the mixing ratio of deionized water and xanthan gum based on sand mass was established at $m_s:m_w:m_b = 100:15:1$ (where m_s is the mass of sand; m_w is the mass of deionized water; and m_b is the mass of xanthan gum biopolymer). The 15% m_w/m_s ratio (water content) was selected to provide sufficient workability at the 1% m_b/m_s concentration while optimizing water usage, given the requirements for retaining wall backfill construction. XG-BPST samples were categorized as either initial (wet) or dehydrated (dry) conditions after a one-day curing period at room temperature (25°C), achieving a final water content below 3%.

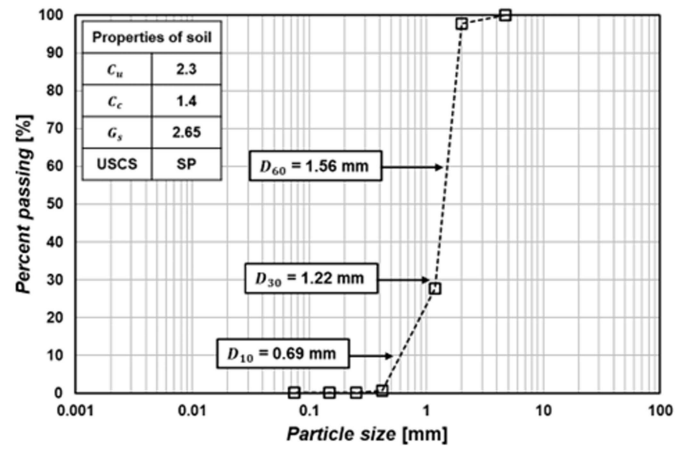


Fig. 1. Particle size distribution of Jumunjin sand.

Table 1. Physical properties of Jumunjin sand

Category	Unit	Test result
Maximum dry unit weight	(kN/m ³)	18.1
Minimum dry unit weight	(kN/m ³)	14.6
Dry unit weight of the experiment	(kN/m ³)	17.2
Relative density	(%)	78.2 (Dense)

Table 2. Result of direct and interface shear test

Conditions	Internal friction angle θ (degrees)	Cohesion (kPa)
Untreated	37	0
XG-BPST (wet)	34	10
XG-BPST (dry)	48	270
Wall friction (δ)	15 (interface)	0

Sand-Xanthan Gum Mixture (XG-BPST): Mechanical Properties

An automated direct shear equipment (HM-5750D.3F, Humboldt Mfg.) was used for both direct and interface shear tests. Table 2 summarizes the shear strength parameters of the soils (i.e., untreated Jumunjin sand, wet XG-BPST sand, and dried XG-BPST sand), measured at a horizontal shear displacement rate of 1 mm/min [ASTM D3080 (ASTM 2012)]. The pseudoplasticity of xanthan gum hydrogel facilitated a lubrication effect between soil particles in the initial (wet) condition of XG-BPST (Stokes et al. 2011), although the change in internal friction angle was negligible. Furthermore, a slight cohesion enhancement effect was noted in the cohesionless sand, resulting in a slight improvement in shear strength. Conversely, in the dehydrated (dry) condition, cured at room temperature (25°C) for a day, inter-particle bridging notably amplified the shear strength (Chang et al. 2015a; Cabalar et al. 2017; Lee et al. 2017).

Geogrid

This study performed tests to verify the behavior of lateral earth pressure when geogrid is embedded in retaining wall backfill or encapsulated in XG-BPST. The use of geogrid, which improves soil binding, was anticipated to increase backfill shear strength through enhanced skin friction. The biaxial geogrid employed

Table 3. Detailed dimensions of the biaxial geogrid

Apertures	Shape	Square
	Size (mm)	32×32
Rib width (mm)	Longitudinal	7.5
	Transverse	6.2
Thickness of transverse ribs (mm)		1.5
Tensile strength (kN/m)		40

consisted of high-strength, low-elongation polyester yarns coated with PVC. Table 3 summarizes the detailed dimensions and physical properties of the geogrid utilized in this study.

Experimental Program

Soil Tank and Measurement System

Fig. 2(a) displays a soil tank with dimensions of 845 mm in length \times 300 mm in width \times 900 mm in height, designed using a transparent acrylic plate, allowing visualization of all test processes from the outside. An internal glass plate minimized friction against the model ground.

The testing wall was designed from seven individual acrylic plates, each with dimensions of 300 mm in length \times 20 mm in width \times 100 mm in height. To avoid eccentricity loading on each plate, two load transducers (total of 14, Bongshin Co., Ltd., Seo-gu, South Korea) and four earth pressure gauges (ZIS I&C Co., Ltd.) were installed to measure lateral earth pressure. The arrangement of

separate plates allows for the measurement of lateral earth pressure variation across each plate and prevents bending moments due to earth pressure. Hinges were installed at the bottom of the wall to enable it rotation (rotation around the base).

Model Ground Formation

The model ground, composed of dry jumunjin sand, was formed using the sand pluviation method (Dave and Dasaka 2012; Gade and Dasaka 2015) with a constant drop height of 700 mm to ensure consistent relative density. Applying this procedure, a dense model ground (total height = 800 mm) with a dry unit weight of 17.2 kN/m^3 and a relative density of 78.2% was formed (Table 1). The rails were isolated from the soil tank to avoid the influence of vibration from storage movement. Rollers were installed to mitigate friction along the rails [Fig. 2(b)].

Model Ground Conditions

The aims of this study were to perform a preliminary feasibility investigation of the lateral earth pressure behavior when XG-BPST was applied to retaining wall backfill. Laboratory tests were performed under strictly controlled conditions, with inter-layer spacing maintained at consistent intervals based on separated and measured plates for earth pressure assessment. XG-BPST layers or geogrids were placed at predetermined positions during the formation of model ground (simulating retaining wall backfill) using the sand pluviation method (with 2, 4, 6 plates for 3 layers and 2, 3, 4, 5, 6 plates for 5 layers, respectively). The test variables were classified as the initial (wet) condition XG-BPST representing immediately after construction, the dehydrated (dry) condition

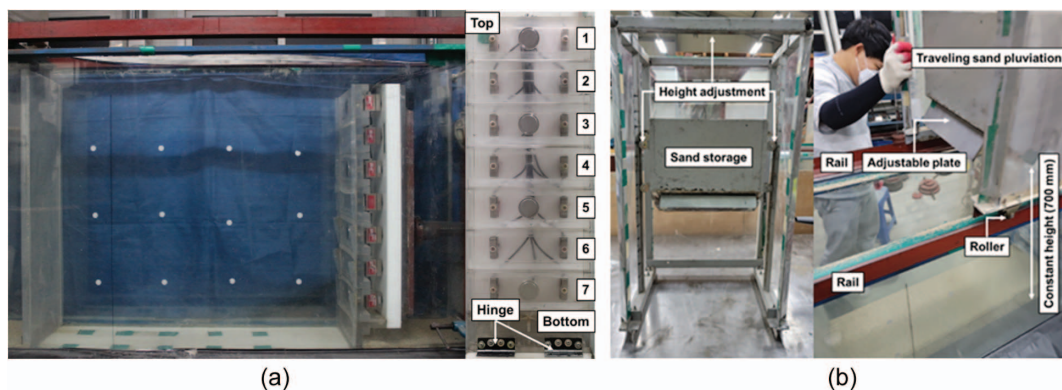


Fig. 2. (Color) Laboratory test apparatus: (a) soil tank and lateral earth pressure measuring plate; and (b) traveling sand pluviation method.

Table 4. Summary of laboratory test conditions

CASE	Biopolymer treated ratio (UT/BP)	Biopolymer hydrogel state (W/D)	Biopolymer treated layer number (L0/L3/L5)	Geogrid number (G0/G3/G5)	Test name	Symbol
1	UT	—	L0	G0	UT-L0-G0	×
2	UT	—	L0	G3	UT-L0-G3	□
3	UT	—	L0	G5	UT-L0-G5	■
4	BP	W	L3	G0	BP(W)-L3-G0	△
5	BP	W	L3	G3	BP(W)-L3-G3	◇
6	BP	D	L3	G0	BP(D)-L3-G0	○
7	BP	W	L5	G0	BP(W)-L5-G0	▲
8	BP	W	L5	G5	BP(W)-L5-G5	◆
9	BP	D	L5	G0	BP(D)-L5-G0	•

Note: UT = Untreated; BP = Biopolymer treated ($m_w/m_s = 15\%$, $m_b/m_s = 1\%$); W = Wet; D = Dry; L0 = 0; L3 = 3; L5 = 5; G0 = 0; G3 = 3; and G5 = 5.

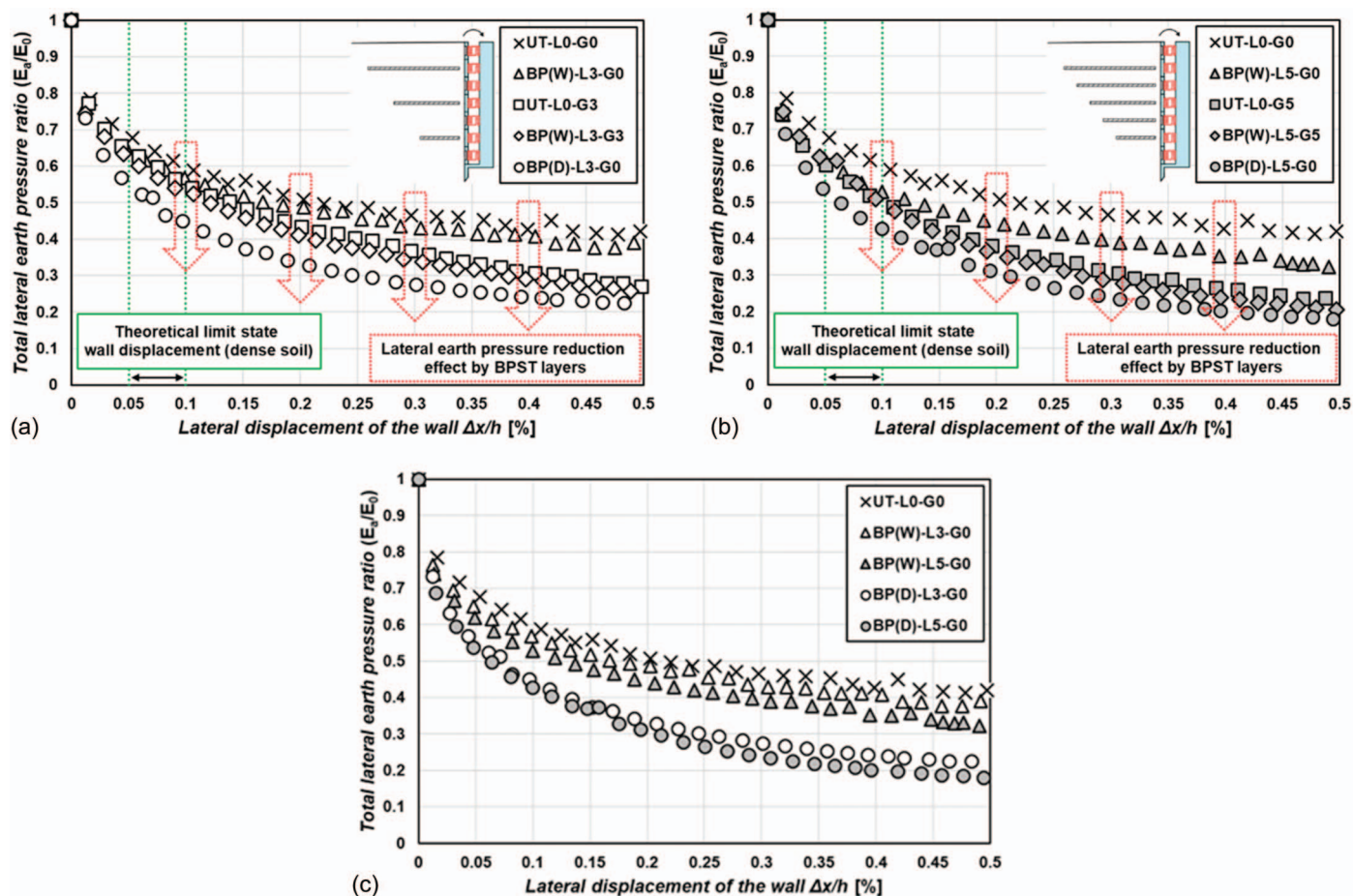


Fig. 4. (Color) Total lateral earth pressure ratio induced by rotation of the wall around the base: (a) three reinforced layers; (b) five reinforced layers; and (c) comparative analysis based on the number of reinforced layers.

In Fig. 4, the XG-BPST layers under initial (wet) condition [BP(W)-L3-G0, BP(W)-L5-G0] showed slight improvement in shear strength, and the quantity of reinforcement was comparatively small relative to the entire model ground; consequently, its impact on the overall lateral earth pressure behavior was negligible. When geogrid is embedded in backfill (UT-L0-G3, UT-L0-G5), the interaction between the soil and the geogrid improves shear strength. Thus, the movement of soil particles, induced by wall rotation, is constrained by the resistance of the geogrid, leading to a reduction in lateral earth pressure. To address the limitations of the initial (wet) condition XG-BPST during early construction phases, a geogrid was encapsulated at the center of the XG-BPST layer [BP(W)-L3-G3, BP(W)-L5-G5], enhancing the cohesion of XG-BPST and achieving an additional reduction in lateral earth pressure compared to the wet condition alone. XG-BPST layers under the dehydrated (dry) condition [BP(D)-L3-G0, BP(D)-L5-G0] significantly increase shear strength, restrict ground deformation induced by wall rotation in the reinforced area, and exert a confining effect on the surrounding ground. This resulted in a substantial reduction in lateral earth pressure compared to the untreated condition.

As the number of reinforced layers increases (thus reducing the spacing between layers), the lateral earth pressure decreases further, though the improvement is negligible [Fig. 4(c)]. The variation caused by reinforcing conditions was more significant than that caused by the number of reinforced layers, and the effect of reducing lateral earth pressure was also developed in nonreinforced areas (Fig. 5). Fig. S1 provides further details on the depth-dependent lateral earth pressure behavior.

The Relationship between Lateral Earth Pressure Behavior and GeoPIV Image Analysis

The GeoPIV image analysis method was used to verify the model ground deformation and the ground movement restriction effect due to the reinforcing condition by wall rotation (active displacement). In Fig. 7, the color bar at the top of the image indicates the displacement range, measured in millimeters. Dotted bars represent XG-BPST layers, while dotted lines indicate geogrids in Fig. 7.

The analysis revealed that in untreated condition (UT-L0-G0), a triangular wedge failure developed as the wall rotated around the base, in line with conventional earth pressure theories. Figs. 4 and 7 indicate that a triangular wedge failure developed within the wall displacement range of $\Delta x/h$ 0.05-0.1% under untreated conditions. Failure was observed at about $\Delta x/h$ 0.1% in other conditions, which was identified as the limit equilibrium (active earth pressure). It was observed that the ground movement was minimally restricted at the reinforced position in the initial (wet) XG-BPST layers. Consequently, compared to the untreated condition, the lateral earth pressure behavior and failure shape were similar. In conditions where shear strength improved, the x-axis movement of soil particles was constrained, and a noticeable suppression of deformation was observed, especially in the dehydrated (dry) XG-BPST condition. Reinforcement increased shear strength, thus reducing soil displacement near the reinforced layers and diminishing the volume of the wedge failure. Since the earth pressure is influenced by the weight of the wedge, a smaller wedge resulted in reduced

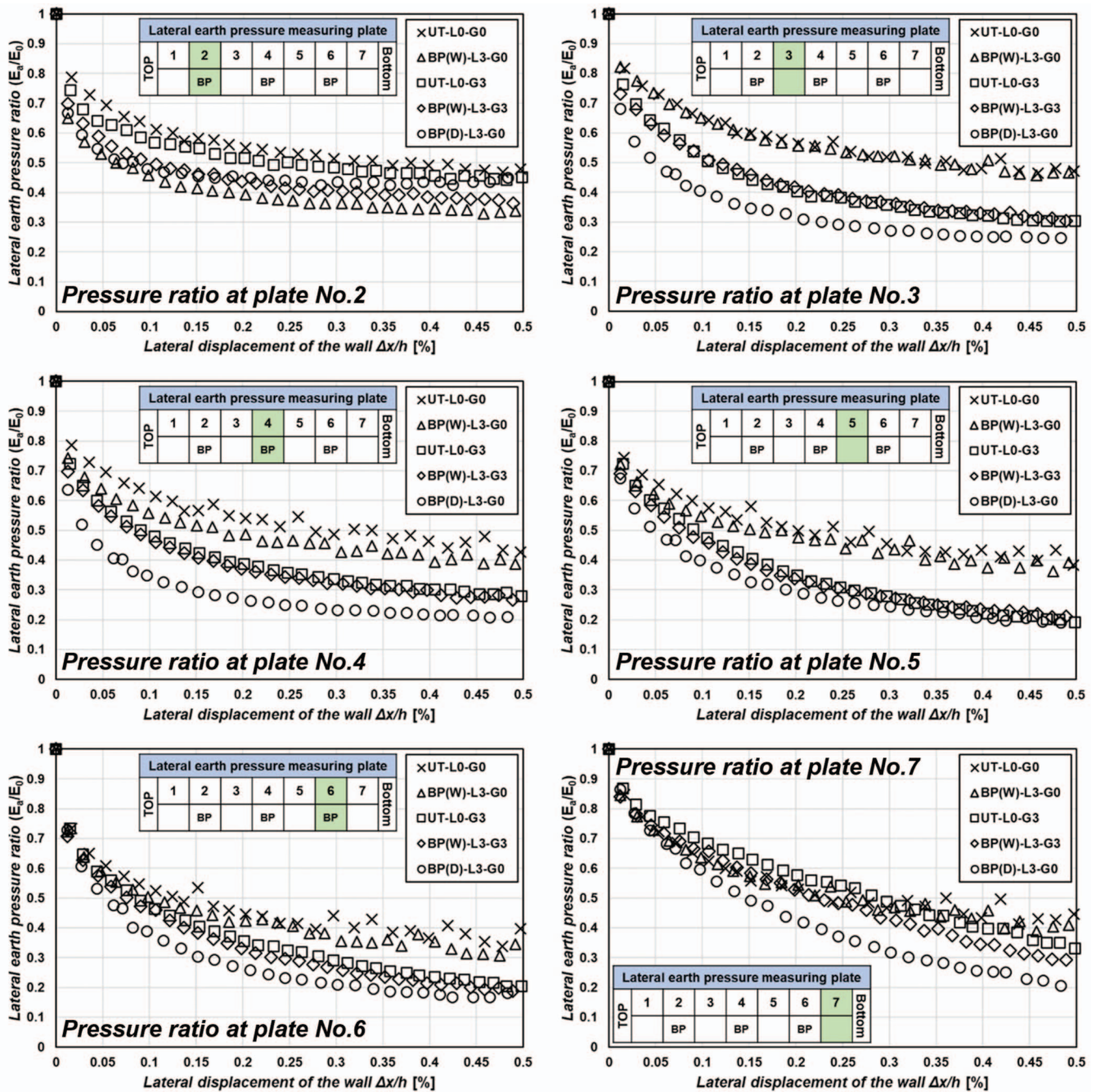


Fig. 5. (Color) Lateral earth pressure ratio at each measurement plate is induced by rotating the base of the wall in the three reinforced layer condition.

lateral earth pressure. Reinforcement proved particularly effective at greater depths with minimal wall displacement, further restraining deformation and reducing lateral earth pressure. Fig. S2 provides more details on GeoPIV image analysis results.

Discussion

Retaining Wall External Stability Affected by XG-BPST Backfill Conditions

Active earth pressure developed at $\Delta x/h$ 0.1% in all laboratory test conditions. Table 5 summarized the lateral earth pressure reduction effect at each wall displacement for all reinforcement conditions as compared to untreated conditions. All reinforcement conditions

indicated reduced earth pressure; the dehydrated (dry) XG-BPST case [i.e., BP(D)-L5-G0] exhibits the greatest reduction in earth pressure.

The active earth pressure reduction effect may help lower retaining wall volume and improve external stability. If an imaginary retaining wall (height of 3 m, width of 2 m, unit weight = 24 kN/m³) is considered, its external stability against sliding and overturning could be evaluated as summarized in Table 6. The scale of the laboratory test results (wall height: 700 mm) was adjusted by applying Coulomb theory to the active earth pressure in the imaginary retaining wall backfill condition. All reinforced conditions showed higher FS (factor of safety) compared to untreated condition (Table 6). AASHTO (2014) recommends minimum FS of 1.5 and 2.0 for sliding and overturning, respectively. The untreated condition seems to be critical, while geogrid reinforcement slightly

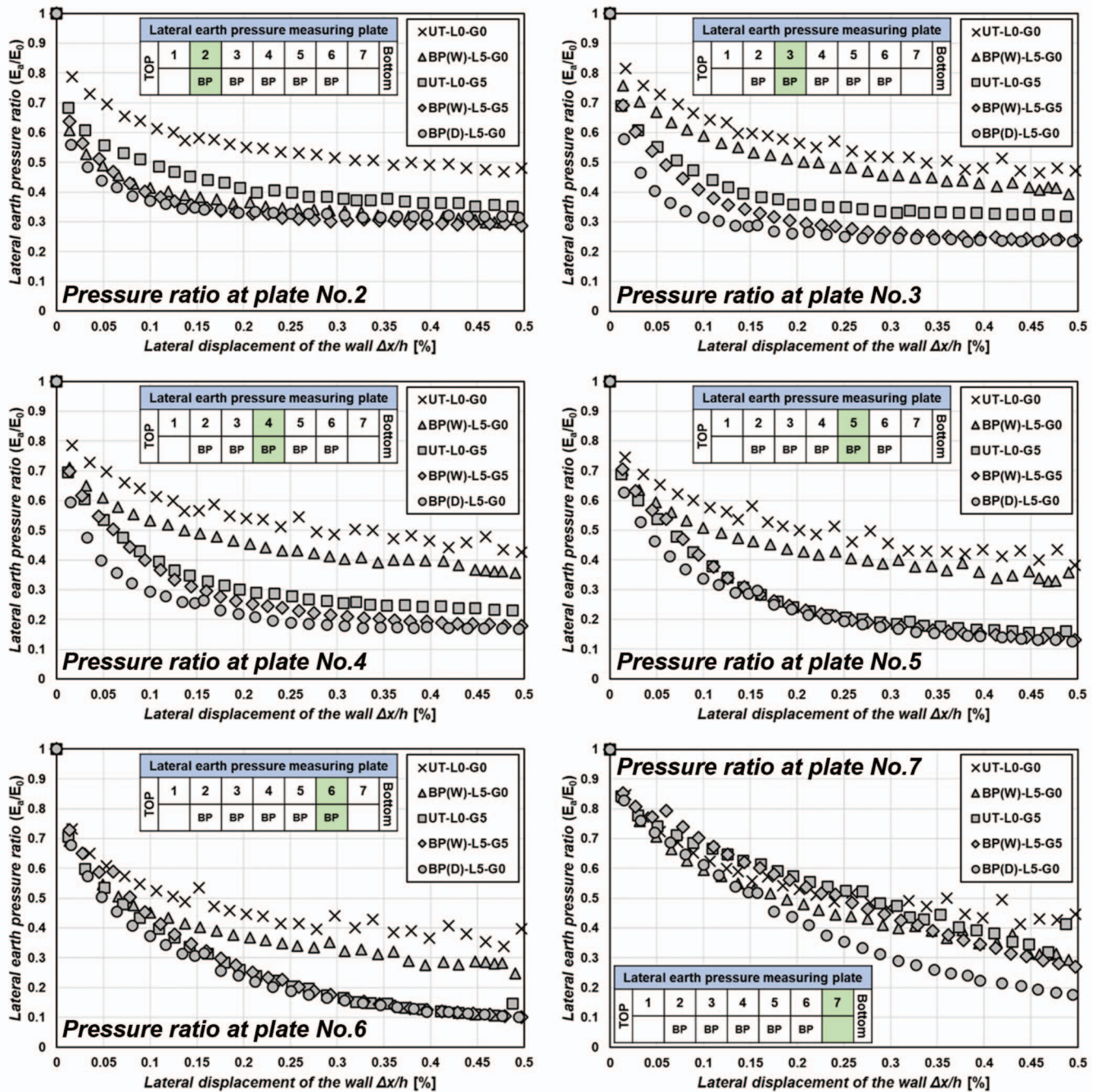


Fig. 6. (Color) Lateral earth pressure ratio at each measurement plate is induced by rotating the base of the wall in the five reinforced layer condition.

improves the FS. However, XG-BPST becomes more sufficient in terms of safety against external stability. Particularly, dehydrated XG-BPST conditions [i.e., BP(D)-L3-G0 and BP(D)-L5-G0] demonstrate a significant reduction in lateral earth pressure which exceeds more than 40%. Therefore, XG-BPST for wall backfill is anticipated to improve the external stability of walls and decrease the structural dimensions required (e.g., wall width) to meet AASHTO's safety criteria.

Response to the Depletion of Natural Construction Resources and Environmental Issues Associated with Cement

This study aims to address environmental issues associated with soil improvement agents in geotechnical engineering by

employing biopolymers to reinforce retaining wall backfill. Cement, commonly used for ground reinforcement, contributes approximately 1 ton of CO₂ emissions per ton produced, accounting for 5%–8% of total global CO₂ emissions (Worrell et al. 2001; Metz et al. 2005; Chu et al. 2009; Oss 2014; Chang et al. 2016b, 2020). Its extensive use in construction is associated with increased urban water runoff, heat island effects, preventing vegetation growth, pH, and demolition problems (Rao et al. 2007; Chang et al. 2016b). Conversely, the production of xanthan gum biopolymer, which consumes about 4.97 kg of CO₂ per kg, is naturally biodegradable and does not adversely affect the geoenvironment or groundwater (Chang et al. 2016b, 2019). Biopolymers are becoming increasingly favored in geotechnical engineering, as they have been proven to develop strength comparable to or exceeding that of cement or other binders at low concentrations.

In practical applications, engineers often prefer locally available cohesive soils to minimize the constraints of granular materials limited availability, transportation costs, shortened construction schedules, and the extensive use of natural construction materials,

which increase costs and raise environmental issues (Christopher and Stulgis 2005; Yang et al. 2019; Guzman and Payano 2023; Razeghi and Ensani 2023; Malek Ghasemi et al. 2024; Saxena et al. 2024). It has been reported that retaining wall backfill

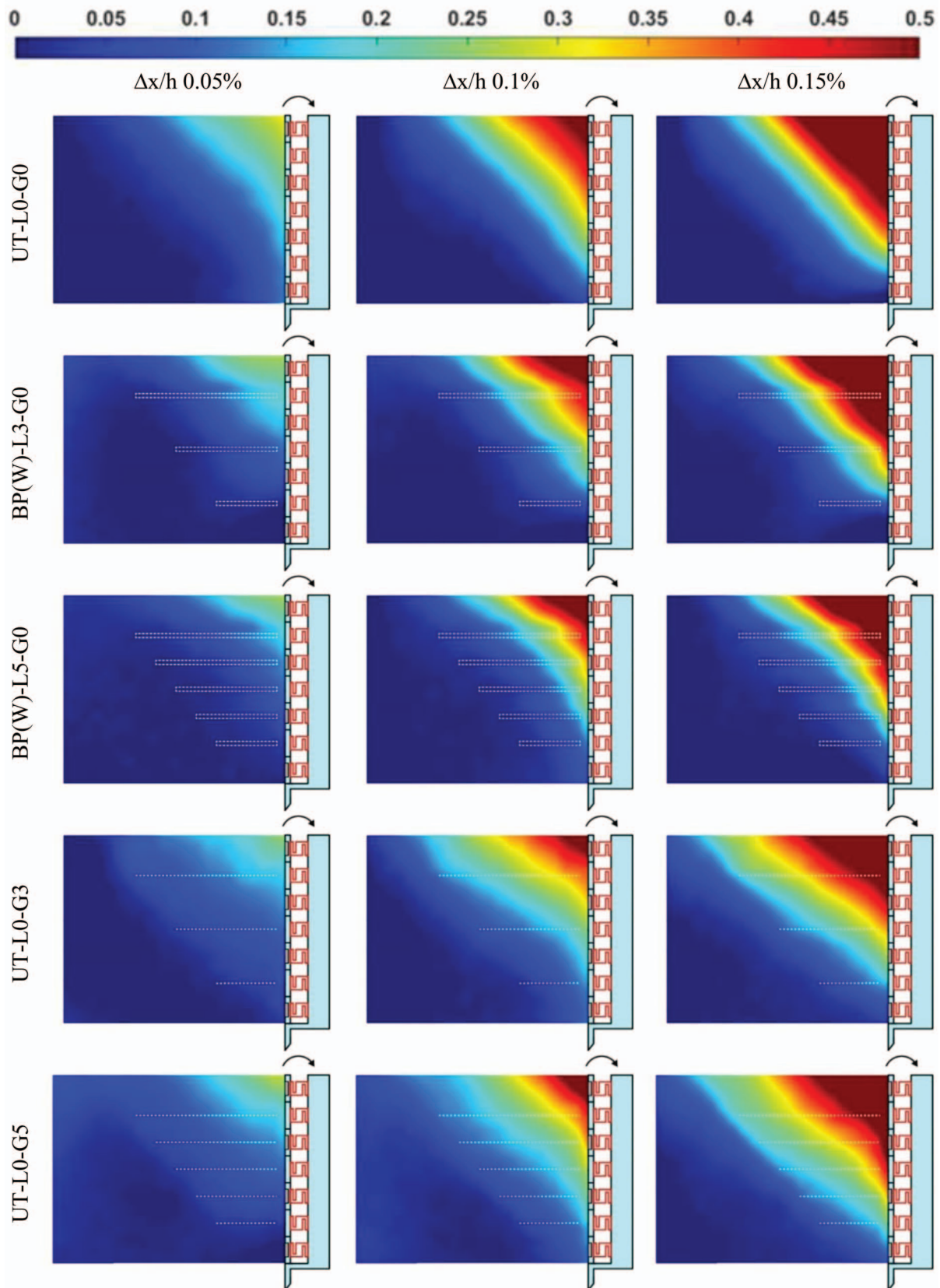


Fig. 7. (Color) GeoPIV image analysis result for x-axis displacement (mm).

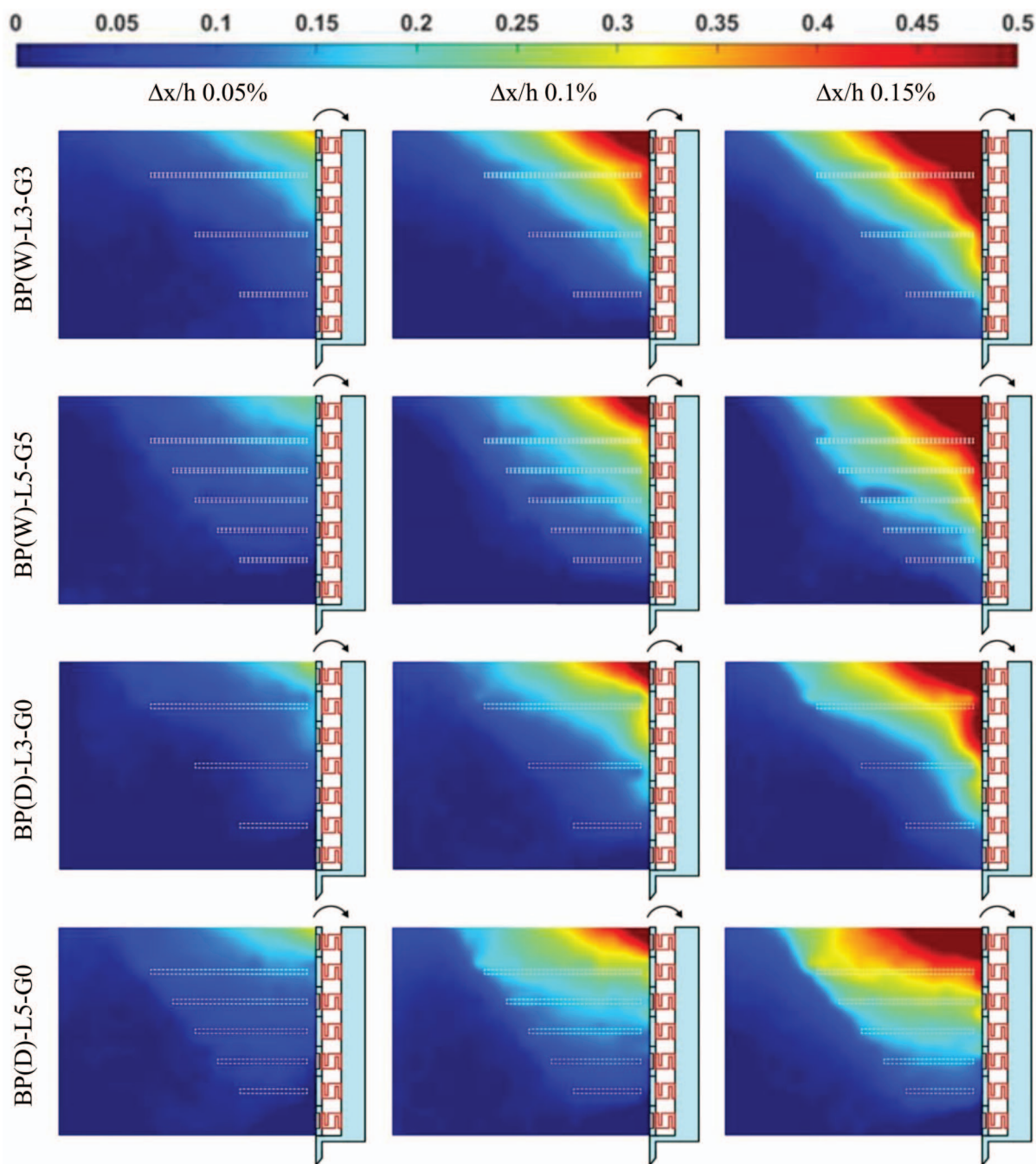


Fig. 7. (Color) (Continued.)

materials can account for up to 50% of total construction costs, with potential savings of 20%–30% achievable by substituting traditional backfill materials with locally cohesive soils (Abdi and Arjomand 2011; Mirzaeifar et al. 2022). Efforts to reduce lateral earth pressure through backfill reinforcement with BPST may enable the utilization of diverse materials, including coarse aggregates, industrial by-products, and locally cohesive soils. This strategy provides several backfill options while addressing environmental issues by reducing resource depletion, enhancing wall stability, and decreasing the volume of retaining walls.

Future Challenges of BPST in Field Applications

Currently, biopolymers are economically unfavorable due to their high global market pricing compared to conventional soil binders

like cement. They are used in various industries (cosmetics, pharmaceuticals, food, etc.) that demand pure and high-quality biopolymers, but they remain uncommon in geotechnical engineering, resulting in high costs for production (Chang et al. 2016b). Recent reports suggest that the unit prices of some biopolymers have decreased as the market expands, and the possibility for rough-quality biopolymers to be applied to geotechnical engineering might lead to future competition (Bajaj et al. 2007; Chang et al. 2015b, 2019). Biopolymer studies are still performed on a laboratory scale, and more advanced studies are needed to develop site implementation methodologies, design standards, and material quality control guidelines, as well as to ensure the durability and reliability of BPST under field conditions (Chang et al. 2020). Although the xanthan gum biopolymer used in this study significantly reduces lateral earth pressure, adequate drainage and maintenance are essential

Table 5. Lateral earth pressure reduction efficiency (%) compared to untreated condition (UT-L0-G0) with wall displacement

Test conditions	Wall displacement $\Delta x/h$		
	0.05%	0.1%	0.15%
UT-L0-G3	4.9%	4.9%	5.9%
UT-L0-G5	8.8%	10.0%	11.8%
BP(W)-L3-G0	4.4%	3.3%	2.9%
BP(W)-L5-G0	7.1%	7.2%	6.8%
BP(W)-L3-G3	6.6%	7.7%	8.5%
BP(W)-L5-G5	7.4%	10.4%	13.1%
BP(D)-L3-G0	13.8%	15.8%	16.6%
BP(D)-L5-G0	16.0%	17.4%	18.5%

Table 6. Factor of safety values for an imaginary retaining wall with different backfill conditions at wall displacement of $\Delta x/h$ 0.1%

Test conditions	Factor of safety (FS)	
	Sliding	Overturing
UT-L0-G0	1.54	3.66
UT-L0-G3	1.55	3.69
UT-L0-G5	1.74	4.11
BP(W)-L3-G0	1.65	3.74
BP(W)-L5-G0	1.69	4.01
BP(W)-L3-G3	1.65	3.90
BP(W)-L5-G5	1.71	4.04
BP(D)-L3-G0	2.20	5.12
BP(D)-L5-G0	2.26	5.26

Note: The minimum FS values are 1.5 and 2.0 for sliding and overturning, respectively according to AASHTO (2014).

due to strength reduction (stability) and durability challenges related to wet backfill conditions. Further studies are needed on the optimal biopolymer content and type, reinforcement length and spacing normalized to the height of the retaining wall, and maintenance and repair after construction to implement retaining wall backfill reinforcement using BPST economically and efficiently.

Conclusions

This study investigated the behavior of lateral earth pressure under backfill reinforcement conditions, utilizing a rotatable wall (rotation around the base) to support sandy soil, through laboratory tests and GeoPIV analysis methods. Based on sand mass, XG-BPST contained 15% deionized water and 1% xanthan gum biopolymer content, and a preliminary feasibility investigation was performed for applying BPST as retaining wall backfill. The effect of lateral earth pressure reduction and subsequent retaining wall stability were analyzed in a backfill reinforced with XG-BPST and geogrid, yielding the following results.

Under all reinforcement conditions, the limit equilibrium developed at a wall displacement of approximately $\Delta x/h$ 0.1%; here, the lateral earth pressure was determined as the active earth pressure. In the initial (wet) condition of XG-BPST, the deformation of the ground in the reinforced area was slightly restricted due to the minimal improvement in shear strength and the limited amount of reinforcement, suggesting that the variation in lateral earth pressure was negligible. To address the challenge of improving the weak shear strength of XG-BPST, a geogrid was encapsulated in the center of the layer. The combined effect of geogrid skin friction and the cohesion of XG-BPST significantly reduced soil particle

movement, leading to further reductions in lateral earth pressure. In the dehydrated (dry) condition XG-BPST, with significantly improved shear strength, effectively decreased lateral earth pressure by constraining ground deformation at the reinforced position and exerting a confining effect on the adjacent soils.

Laboratory test results facilitated external stability (sliding, overturning) analysis by reducing the active earth pressure using an imaginary retaining wall. In the dehydrated (dry) condition of XG-BPST, the FS was improved by at least 40% compared to the untreated condition, and the minimum width of the retaining wall required to meet the FS guidelines also decreased, allowing for economical design.

The findings of this study provide various options for utilizing backfill materials to save cost, improve external stability, and decrease volume in response to economic design and environmental concerns. However, further studies are necessary to determine the optimal biopolymer content and type, reinforcement length and spacing, and postconstruction maintenance and repair strategies for practical improvement of retaining wall backfill using BPST.

Data Availability Statement

All data, models, and code generated or used during the study appear in the published article.

Acknowledgments

This work was supported by National Research Foundation of Korea (NRF) Grant No. 2022R1A2C2091517 funded by the Korea government (MSIT).

Supplemental Materials

Figs. S1 and S2 are available online in the ASCE Library (www.ascelibrary.org).

References

- AASHTO. 2014. *AASHTO LRFD bridge design specifications*. 7th ed. Washington, DC: AASHTO.
- Abdi, M. R., and M. A. Arjomand. 2011. "Pullout tests conducted on clay reinforced with geogrid encapsulated in thin layers of sand." *Geotext. Geomembr.* 29 (6): 588–595. <https://doi.org/10.1016/j.geotextmem.2011.04.004>.
- ASTM. 2012. *Standard test method for direct shear test of soils under consolidated drained conditions*. ASTM D3080-04. West Conshohocken, PA: ASTM.
- Azzam, S., and S. Abdelsalam. 2015. "EPS geofoam to reduce lateral earth pressure on rigid walls." In *Proc., Int. Conf. on Advances in Structural and Geotechnical Engineering*, 6–9. Hurghada, Egypt: ICASGE.
- Bajaj, I. B., S. A. Survase, P. S. Saudagar, and R. S. Singhal. 2007. "Gellan gum: Fermentative production, downstream processing and applications." *Food Technol. Biotechnol.* 45 (4): 341–354.
- Cabalar, A. F., M. Wiszniewski, and Z. Skutnik. 2017. "Effects of xanthan gum biopolymer on the permeability, odometer, unconfined compressive and triaxial shear behavior of a sand." *Soil Mech. Found. Eng.* 54 (5): 356–361. <https://doi.org/10.1007/s11204-017-9481-1>.
- Cecich, V., L. Gonzales, A. Hoisaeter, J. Williams, and K. Reddy. 1996. "Use of shredded tires as lightweight backfill material for retaining structures." *Waste Manage. Res.* 14 (5): 433–451. <https://doi.org/10.1177/0734242X9601400503>.
- Chang, I., J. Im, and G.-C. Cho. 2016a. "Geotechnical engineering behaviors of gellan gum biopolymer treated sand." *Can. Geotech. J.* 53 (10): 1658–1670. <https://doi.org/10.1139/cgj-2015-0475>.

- Chang, I., J. Im, and G.-C. Cho. 2016b. "Introduction of microbial biopolymers in soil treatment for future environmentally-friendly and sustainable geotechnical engineering." *Sustainability* 8 (3): 251. <https://doi.org/10.3390/su8030251>.
- Chang, I., J. Im, A. K. Prasadhi, and G.-C. Cho. 2015a. "Effects of Xanthan gum biopolymer on soil strengthening." *Constr. Build. Mater.* 74 (Jan): 65–72. <https://doi.org/10.1016/j.conbuildmat.2014.10.026>.
- Chang, I., M. Lee, and G.-C. Cho. 2019. "Global CO₂ emission-related geotechnical engineering hazards and the mission for sustainable geotechnical engineering." *Energies* 12 (13): 2567. <https://doi.org/10.3390/en12132567>.
- Chang, I., M. Lee, A. T. P. Tran, S. Lee, Y.-M. Kwon, J. Im, and G.-C. Cho. 2020. "Review on biopolymer-based soil treatment (BPST) technology in geotechnical engineering practices." *Transp. Geotech.* 24 (Sep): 100385. <https://doi.org/10.1016/j.trgeo.2020.100385>.
- Chang, I., A. K. Prasadhi, J. Im, and G.-C. Cho. 2015b. "Soil strengthening using thermo-gelation biopolymers." *Constr. Build. Mater.* 77 (Feb): 430–438. <https://doi.org/10.1016/j.conbuildmat.2014.12.116>.
- Chang, M. F. 1997. "Lateral earth pressures behind rotating walls." *Can. Geotech. J.* 34 (4): 498–509. <https://doi.org/10.1139/t97-016>.
- Chauhan, V., R. Khan, and S. Dasaka. 2016a. "Reduction of lateral earth pressure acting on non-yielding retaining wall using relief shelves." In *Proc., Indian Geotechnical Conf.*, New Delhi, India: Indian Geotechnical Society.
- Chauhan, V. B., S. M. Dasaka, and V. K. Gade. 2016b. "Investigation of failure of a rigid retaining wall with relief shelves." *Jpn. Geotech. Soc.* 2 (73): 2492–2497. <https://doi.org/10.3208/jgssp.TC302-02>.
- Chauhan Vinay, B., and S. M. Dasaka. 2018. "Performance of a rigid retaining wall with relief shelves." *J. Perform. Constr. Facil.* 32 (3): 04018021. [https://doi.org/10.1061/\(ASCE\)CF.1943-5509.0001161](https://doi.org/10.1061/(ASCE)CF.1943-5509.0001161).
- Christopher, B. R., and R. P. Stulgis. 2005. "Low permeable backfill soils in geosynthetic reinforced soil walls: State-of-the-practice in North America." In *Proc., North American Geo-synthetics Conf. (NAGS 2005)*, 14–16. Las Vegas: NAGS.
- Chu, J., S. Varaksin, U. Klotz, and P. Mengé. 2009. "Construction processes." In *Proc., 17th Int. Conf. on Soil Mechanics and Geotechnical Engineering (Volumes 1, 2, 3 and 4)*, 3006–3135. Amsterdam, Netherlands: IOS Press. <https://doi.org/10.3233/978-1-60750-031-5-3006>.
- Dave, T. N., and S. Dasaka. 2012. "Assessment of portable traveling pluviator to prepare reconstituted sand specimens." *Geomech. Eng.* 4 (2): 79–90. <https://doi.org/10.12989/gae.2012.4.2.079>.
- Djadouni, H., H. Trouzine, A. Gomes Correia, and T. F. Miranda. 2021. "2D numerical analysis of a cantilever retaining wall backfilled with sand–tire chips mixtures." *Eur. J. Environ. Civ. Eng.* 25 (6): 1119–1135. <https://doi.org/10.1080/19648189.2019.1570870>.
- Ertugrul, O. L., and A. C. Trandafir. 2011. "Reduction of lateral earth forces acting on rigid nonyielding retaining walls by EPS geofoam inclusions." *J. Mater. Civ. Eng.* 23 (12): 1711–1718. [https://doi.org/10.1061/\(ASCE\)MT.1943-5533.0000348](https://doi.org/10.1061/(ASCE)MT.1943-5533.0000348).
- Ertugrul, O. L., and A. C. Trandafir. 2013. "Lateral earth pressures on flexible cantilever retaining walls with deformable geofoam inclusions." *Eng. Geol.* 158 (May): 23–33. <https://doi.org/10.1016/j.enggeo.2013.03.001>.
- Fang, Y. S., T. J. Chen, and B. F. Wu. 1994. "Earth pressures under general wall movements." *Geotech. Eng.* 24 (2): 113–131. [https://doi.org/10.1061/\(ASCE\)0733-9410\(1994\)120:8\(1307\)](https://doi.org/10.1061/(ASCE)0733-9410(1994)120:8(1307)).
- Fang, Y. S., and I. Ishibashi. 1986. "Static earth pressures with various wall movements." *J. Geotech. Eng.* 112 (3): 317–333. [https://doi.org/10.1061/\(ASCE\)0733-9410\(1986\)112:3\(317\)](https://doi.org/10.1061/(ASCE)0733-9410(1986)112:3(317)).
- Gade, V. K., and S. M. Dasaka. 2015. "Development of a mechanized traveling pluviator to prepare reconstituted uniform sand specimens." *J. Mater. Civ. Eng.* 28 (2): 04015117. [https://doi.org/10.1061/\(ASCE\)MT.1943-5533.0001396](https://doi.org/10.1061/(ASCE)MT.1943-5533.0001396).
- Gade, V. K., and S. M. Dasaka. 2022. "Short-and long-term behavior of EPS geofoam in reduction of lateral earth pressure on rigid retaining wall subjected to surcharge loading." *Geotext. Geomembr.* 50 (5): 868–880. <https://doi.org/10.1016/j.geotexmem.2022.05.002>.
- Guzman, I. L., and C. Payano. 2023. "Use of repurposed whole textile for enhancement of pavement soils." *Int. J. Geo-Eng.* 14 (1): 12. <https://doi.org/10.1186/s40703-023-00190-1>.
- Han, Z., W.-L. Zou, Z.-Q. Ying, H.-P. Feng, and G.-Q. Yang. 2023. "A semi-empirical approach for estimating the lateral earth pressure on rigid retaining walls with EPS inclusions in cohesionless soils." *Transp. Geotech.* 39 (Mar): 100937. <https://doi.org/10.1016/j.trgeo.2023.100937>.
- Horvath, J. S. 1997. "The compressible inclusion function of EPS geofoam." *Geotext. Geomembr.* 15 (1–3): 77–120. [https://doi.org/10.1016/S0266-1144\(97\)00008-3](https://doi.org/10.1016/S0266-1144(97)00008-3).
- Ikizler, S. B., M. Aytekin, and E. Nas. 2008. "Laboratory study of expanded polystyrene (EPS) geofoam used with expansive soils." *Geotext. Geomembr.* 26 (2): 189–195. <https://doi.org/10.1016/j.geotexmem.2007.05.005>.
- Kaneda, K., H. Hazarika, and H. Yamazaki. 2018. "Examination of earth pressure reduction mechanism using tire-chip inclusion in sandy backfill via numerical simulation." *Soils Found.* 58 (5): 1272–1281. <https://doi.org/10.1016/j.sandf.2018.06.002>.
- Khajeh, A., R. Jamshidi Chenari, and M. Payan. 2020. "A review of the studies on soil-EPS composites: Beads and blocks." *Geotech. Geol. Eng.* 38 (Aug): 3363–3383. <https://doi.org/10.1007/s10706-020-01252-2>.
- Khan, R., V. Chauhan, and D. Murty. 2016. "Reduction of lateral earth pressure on retaining wall using relief shelf: A numerical study." In *Proc., Int. Conf. on Soil and Environment*, 1–8. New Delhi, India: Indian Geotechnical Society.
- Khosravi, M. H., T. Pipatponga, and J. Takemura. 2013. "Experimental analysis of earth pressure against rigid retaining walls under translation mode." *Geotechnique* 63 (12): 1020–1028. <https://doi.org/10.1680/geot.12.P.021>.
- Lee, S., I. Chang, M. Chung, Y. Kim, and J. Kee. 2017. "Geotechnical shear behavior of xanthan gum biopolymer treated sand from direct shear testing." *Geomech. Eng.* 12 (5): 831–847. <https://doi.org/10.12989/gae.2017.12.5.831>.
- Malek Ghasemi, S., S. M. Binesh, and P. Tabatabaie Shourijeh. 2024. "Improving clay-geogrid interaction: Enhancing pullout resistance with recycled concrete aggregate encapsulation." *Geotext. Geomembr.* 52 (6): 1145–1160. <https://doi.org/10.1016/j.geotexmem.2024.07.010>.
- Metz, B., O. Davidson, H. De Coninck, M. Loos, and L. Meyer. 2005. *IPCC special report on carbon dioxide capture and storage*. Cambridge, UK: Cambridge University Press.
- Mirzaeifar, H., K. Hatami, and M. R. Abdi. 2022. "Pullout testing and Particle Image Velocimetry (PIV) analysis of geogrid reinforcement embedded in granular drainage layers." *Geotext. Geomembr.* 50 (6): 1083–1109. <https://doi.org/10.1016/j.geotexmem.2022.06.008>.
- Moon, I.-J., B.-I. Kim, W.-K. Yoo, and Y.-S. Park. 2013. "Model tests for measurement of lateral earth pressure on retaining wall with the relieving platform using jumoonjin sand." *J. Korea Acad. Ind. Cooperation Soc.* 14 (11): 5923–5929. <https://doi.org/10.5762/KAIS.2013.14.11.5923>.
- Ni, P., G. Mei, and Y. Zhao. 2016. "Displacement-dependent earth pressures on rigid retaining walls with compressible geofoam inclusions: Physical modeling and analytical solutions." *Int. J. Geomech.* 17 (6): 04016132. [https://doi.org/10.1061/\(ASCE\)GM.1943-5622.0000838](https://doi.org/10.1061/(ASCE)GM.1943-5622.0000838).
- Niedostatkiewicz, M., D. Lesniewska, and J. Tejchman. 2011. "Experimental analysis of shear zone patterns in cohesionless for earth pressure problems using particle image velocimetry." *Strain* 47 (Dec): 218–231. <https://doi.org/10.1111/j.1475-1305.2010.00761.x>.
- Oss, H. 2014. *Cement statistics and information*. Reston, VA: USGS.
- Patel, S., and K. Deb. 2020. "Study of active earth pressure behind a vertical retaining wall subjected to rotation about the base." *Int. J. Geomech.* 20 (4): 04020028. [https://doi.org/10.1061/\(ASCE\)GM.1943-5622.0001639](https://doi.org/10.1061/(ASCE)GM.1943-5622.0001639).
- Rao, A., K. N. Jha, and S. Misra. 2007. "Use of aggregates from recycled construction and demolition waste in concrete." *Resour. Conserv. Recycl.* 50 (1): 71–81. <https://doi.org/10.1016/j.resconrec.2006.05.010>.
- Razeghi, H. R., and A. Ensani. 2023. "Clayey sand soil interactions with geogrids and geotextiles using large-scale direct shear tests." *Int. J. Geosynth. Ground Eng.* 9 (2): 24. <https://doi.org/10.1007/s40891-023-00443-0>.
- Reddy, S. B., and A. M. Krishna. 2015. "Recycled tire chips mixed with sand as lightweight backfill material in retaining wall applications:

- An experimental investigation." *Int. J. Geosynth. Ground Eng.* 1 (Dec): 1. <https://doi.org/10.1007/s40891-015-0036-0>.
- Rui, R., R.-J. Xia, J. Han, Y.-Q. Ye, X. Miao, and M. Elabd. 2024. "Experimental investigations of lateral earth pressures behind rigid retaining walls under different displacement modes." *Acta Geotech.* 19 (5): 2545–2562. <https://doi.org/10.1007/s11440-023-02068-z>.
- Saxena, S., L. B. Roy, P. K. Gupta, V. Kumar, and P. Paramasivam. 2024. "Model tests on ordinary and geosynthetic encased stone columns with recycled aggregates as filler material." *Int. J. Geo-Eng.* 15 (1): 1. <https://doi.org/10.1186/s40703-023-00202-0>.
- Stanier, S. A., J. Blaber, W. A. Take, and D. J. White. 2016. "Improved image-based deformation measurement for geotechnical applications." *Can. Geotech. J.* 53 (5): 727–739. <https://doi.org/10.1139/cgj-2015-0253>.
- Stokes, J. R., L. Macakova, A. Chojnicka-Paszun, C. G. de Kruijff, and H. H. J. de Jongh. 2011. "Lubrication, adsorption, and rheology of aqueous polysaccharide solutions." *Langmuir* 27 (7): 3474–3484. <https://doi.org/10.1021/la104040d>.
- Tweedie, J. J., D. N. Humphrey, and T. C. Sandford. 1998. "Tire shreds as lightweight retaining wall backfill: Active conditions." *J. Geotech. Geoenviron. Eng.* 124 (11): 1061–1070. [https://doi.org/10.1061/\(ASCE\)1090-0241\(1998\)124:11\(1061\)](https://doi.org/10.1061/(ASCE)1090-0241(1998)124:11(1061)).
- White, D., and W. Take. 2002. *Particle image velocimetry (PIV) software for use in geotechnical testing*. Cambridge, UK: Univ. of Cambridge, Dept. of Engineering.
- Worrell, E., L. Price, N. Martin, C. Hendriks, and L. O. Meida. 2001. "Carbon dioxide emissions from the global cement industry." *Annu. Rev. Energy Environ.* 26 (1): 303–329. <https://doi.org/10.1146/annurev.energy.26.1.303>.
- Xu, L., H.-B. Chen, F.-Q. Chen, Y.-J. Lin, and C. Lin. 2022. "An experimental study of the active failure mechanism of narrow backfills installed behind rigid retaining walls conducted using Geo-PIV." *Acta Geotech.* 17 (9): 4051–4068. <https://doi.org/10.1007/s11440-021-01438-9>.
- Yang, K.-H., J. N. Thuo, J.-W. Chen, and C.-N. Liu. 2019. "Failure investigation of a geosynthetic-reinforced soil slope subjected to rainfall." *Geosynth. Int.* 26 (1): 42–65. <https://doi.org/10.1680/jgein.18.00035>.